

DESY Summer Student Program 2011

Simulations of beam emission measurements at PITZ¹

Javier Fernández Castañón²

Universidad de Oviedo (Spain)

supervised by Mikhail Krasilnikov and Martin Khojayan

DESY PITZ Group

Platanenalle 6, Zeuthen, 15738, Germany

Abstract

Detailed studies on beam measurements have been made at PITZ. Differences observed in the emittance between experimental and simulated results are studied using ASTRA simulations. The Schottky effect applied on a semiconductor surface is considered to justify the discrepancies obtained in the simulations as well as the emission process. Laser energy scans and experimental phase scans are also considered.



¹Photo Injector Test Facility at DESY in Zeuthen

²javier.fernandez.castanon@desy.de
UO204021@uniovi.es

1. Introduction

The production of high brightness electron beams is a key technology that allows many of today's advanced beam applications, such as Free-Electron Lasers (FELs) or linear colliders. The aim of PITZ is to develop electron sources which can produce high density electron beams with small transverse emittance and with short bunch length.

In order to optimize and characterize the beam quality, ASTRA code[1] was developed to simulate electron beam properties from the photocathode.[2]

ASTRA (A Space Charge Tracking Algorithm) package allows generating an initial particle distribution. It also tracks the particles under the influence of external and internal fields and presents several different plots with the intention of better understanding.

At the first part of this report are introduced the mean physical concepts, which are necessary to understand in depth. Then the motivations and the first simulations are analyzed and finally the comparisons with the experimental results are presented, just before the conclusions.

2. Objectives

Following in the line of the aforementioned discrepancies when comparing experimental results and simulations, it is intended, by the use of ASTRA code; faithfully represent what is happening, so simulations fit acceptably with measurements. Values of the parameters that meet these requirements may be used for future actions so as to optimize beam quality.

Therefore, it is important to understand how Schottky effect, among others, is able to affect photoemission process, as well as to what extent the emission is responsible for the discrepancies found.

3. Physics of electron emission[3]

Before starting development of my analytical work itself is considered appropriate to introduce the main theoretical concepts to which reference will be made throughout the article.

3.1. Field emission from semiconductor photocathodes

In photocathode rf³ guns, the cathode emits electrons when illuminated by the drive-laser. The figures of merit for the photocathode characterization are the operative lifetime, the achievable current density, the extracted charge, the quantum efficiency (QE), and the uniformity of the emissive layer. At present the best photocathode for PITZ is thought to be Cesium Telluride (Cs₂Te) for the following reasons: Cs₂Te is less sensitive to gas exposure than other alkali semiconductors, it can generate a high current density electron bunch when deposited on a metallic substrate, and it can also provide a reasonable QE of the order of 1%. Cs₂Te has a band gap energy of 3.3 eV and an electron affinity of 0.2 eV. Cs₂Te is almost "blind" to visible light, therefore UV light is required for photoemission and dark current photoemitted from the cathode by visible light background is negligible.

In semiconductors at room temperature, the Fermi level is located in the forbidden band between valence and conduction bands and the conduction band is rarely occupied. Therefore, electrons can be emitted only from the valence band. In some cases the conduction band could be empty and therefore field emission occurs by tunneling from the valence band to the vacuum if the applied field is high enough.

³radio frequency gun L-band (1.3 GHz)

3.2. Photoemission

The process of photoemission can be concisely described in a three-step model

- (1) the absorbed photons deliver their energy to electrons inside the material;
- (2) the energized electrons move through the material to the surface, losing some energy;
- (3) the electrons escape over the surface barrier (electrons affinity) into the vacuum.

Not all photons incident on a photoemissive material cause electron emission. When photons strike a photoemissive material, some part is reflected from the surface and only a fraction can impart the energy to the electrons in the material. The ratio of the number of emitted electrons to the number of incident photons is defined as the quantum efficiency (QE). The QE is always less than unity because the photon absorption is less than one, some fraction of energy is lost at each stage of the photoemission process and the generated electrons can move into the material⁴. Dominant factors determining the QE are the wavelength of the incident light and the composition, thickness, and topology of the photoemissive material. Metals are highly reflective; however semiconductors or insulators have a low reflection coefficient and absorb the photon energy more effectively.

3.3. Secondary emission

When a primary electron strikes a solid material, it may penetrate the surface and generate secondary electrons. The origin of secondary electrons is separated into the following three categories: When the primary electron is reflected off the surface, it is called “back-scattered electron”. If the electron penetrates the surface and scatters off one or more atoms and is reflected back out, it is a “rediffused electron”. If the electron interacts inelastically with the material and releases more electrons, “true secondary electrons” are generated. In future graphics will be made allusion to this concept because it has been experimentally obtained, which does not occur in the simulations. Nevertheless, the work has been focused on first emission process.

3.4. Schottky effect

Schottky effect can be understood as a reduction in the work function of electrons emitted from solids that occurs under the influence of an applied electric field that accelerates the wavelength. This effect occurs in electric fields that are strong enough to neutralize the space charge at the surface of the emitter. With an increase of the rf field strength at the Cs₂Te cathode, electrons. The Schottky effect is exhibited as an increase in saturation thermionic current, a decrease in surface ionization energy and a shift of the photoelectric threshold toward longer a potential barrier defined by the electron affinity E_A is lowered and, as the result, the probability of electron extraction is increased.

In *Astra* the charge of a particle is determined at the time of its emission as:

$Q = Q_0 + \text{SRT_Q_Schottky} \cdot \sqrt{E} + Q_Schottky \cdot E$; where E is the combined (external plus space charge) longitudinal electric field in the center of the cathode. The charge Q_0 is the charge of the particle as defined in the input distribution (eventually rescaled according to the parameter Q_bunch) and SRT_Q_Schottky and $Q_Schottky$ describe the field dependent emission process.

4. Motivations

The main motivations of this work are marked by the objectives set out above. The large

⁴This is true except if secondary electrons are generated during the photoemission process inside the material at very high photon energies.

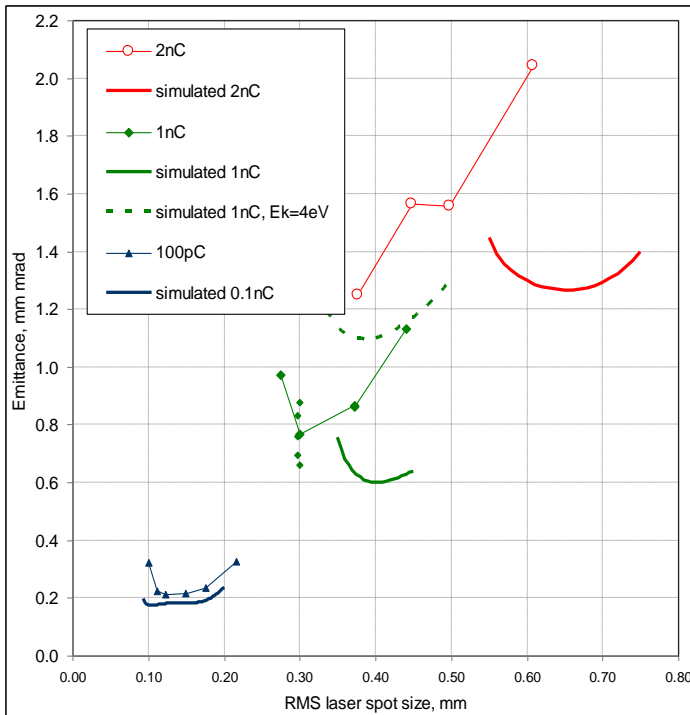


Figure 1: Measured and simulated emittance

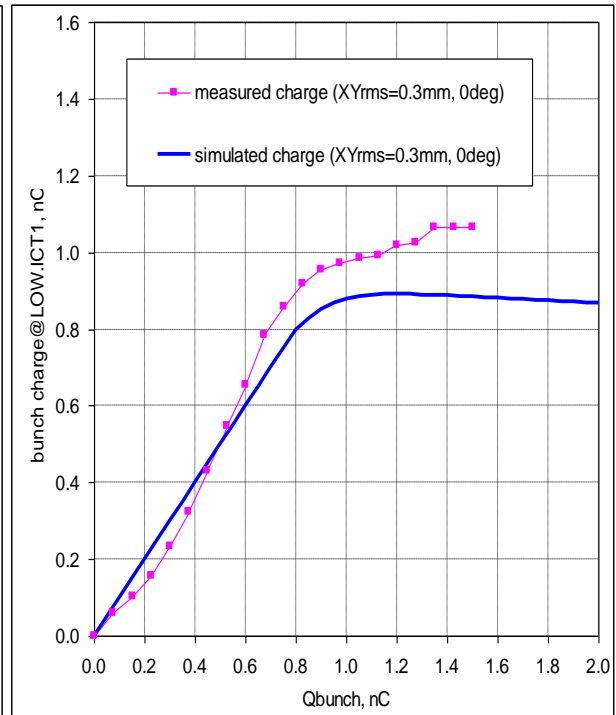


Figure 2: Measured and simulated laser intensity scan

differences found when comparing experimental results with simulations about beam emittance, especially when charge values are increased (see Figure 1), forces us to find the reason why this happens. Similarly, it is necessary to understand the origin of the differences in values obtained for the highest beam charges as well as why the experimental saturation level increases whereas the simulated charge even goes slightly down while the laser intensity (Q_{bunch}) increases (Figures 2 and 3) due to the limitation from the space charge forces at the cathode.

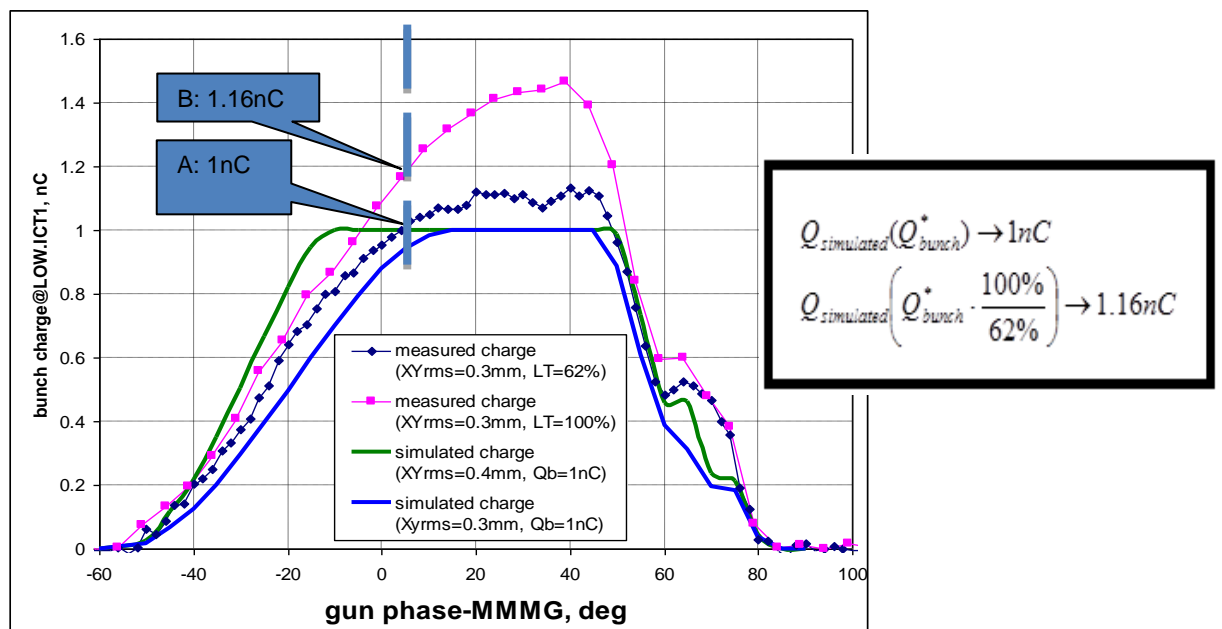


Figure3: Measured and simulated Schottky scans

5. Firsts steps with ASTRA

In order to getting involved with the mentioned ASTRA code was important to learn how to create and modify simulations obtained, as well as interpreting the results.

The steps that were followed are explained below.

5.1. Phase Scans

From given initial bunch charge values and the respective values of Schottky charge⁵ (*Figure 4 and Table 1*), which were experimentally obtained, is carried out a study on the resultant electron beam charge as a function of the gun launch phase.

The phase values are considered between -60 and 90 degrees with a step of 5 degrees while the bunch charge (Q_{bunch}) is modified between 0.1 and 1 nC with a step of 0.1 nC.

The resultant plot is shown in *Figure 5*.

Nr	Q_{bunch} (nC)	Q_{Schottky} (nC)
1	0.1	0.089705212
2	0.2	0.082543967
3	0.3	0.073541731
4	0.4	0.061691542
5	0.5	0.049348598
6	0.6	0.046783626
7	0.7	0.044964029
8	0.8	0.042900043
9	0.9	0.039007448
10	1	0.034852099

Table 1

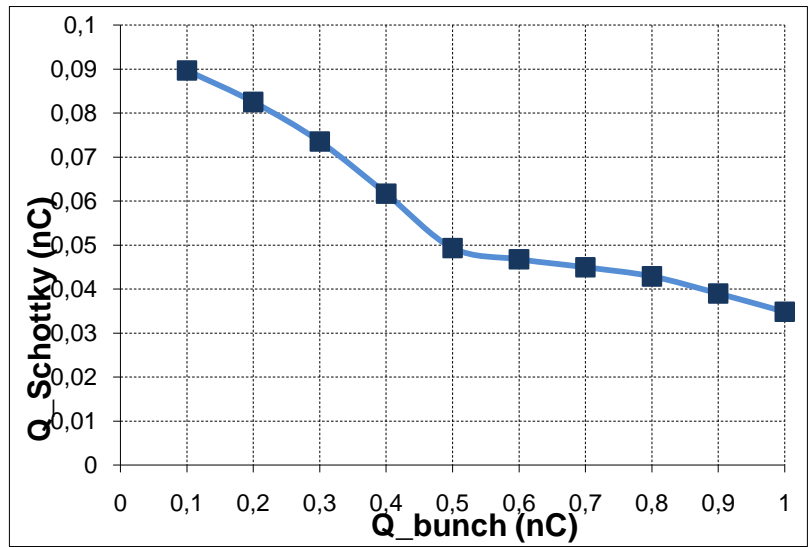


Figure 4: Relationship between the values of Q_{bunch} and Q_{Schottky} obtained from simulations.

The numbers which appear in the legend refer to those shown in the *Table 1*.

In this last figure we can see how the width of all the graphs is exactly the same. The only appreciable difference in the shape of each one is observed in the maximum value of the final electron bunch charge (Q_{tot}).

However, the fact of modify concurrently Q_{bunch} and Q_{schottky} does not make recognize which is the responsible of this behavior possible.

In our attempt to try to represent as closely as possible the physical phenomenon that takes place and was obtained experimentally we remain always constant one of the parameters. So is possible understand the relevance of the others.

⁵Schottky Charge (Q_{Schottky}) is defined as a linear variation of the bunch charge with the field on the cathode.

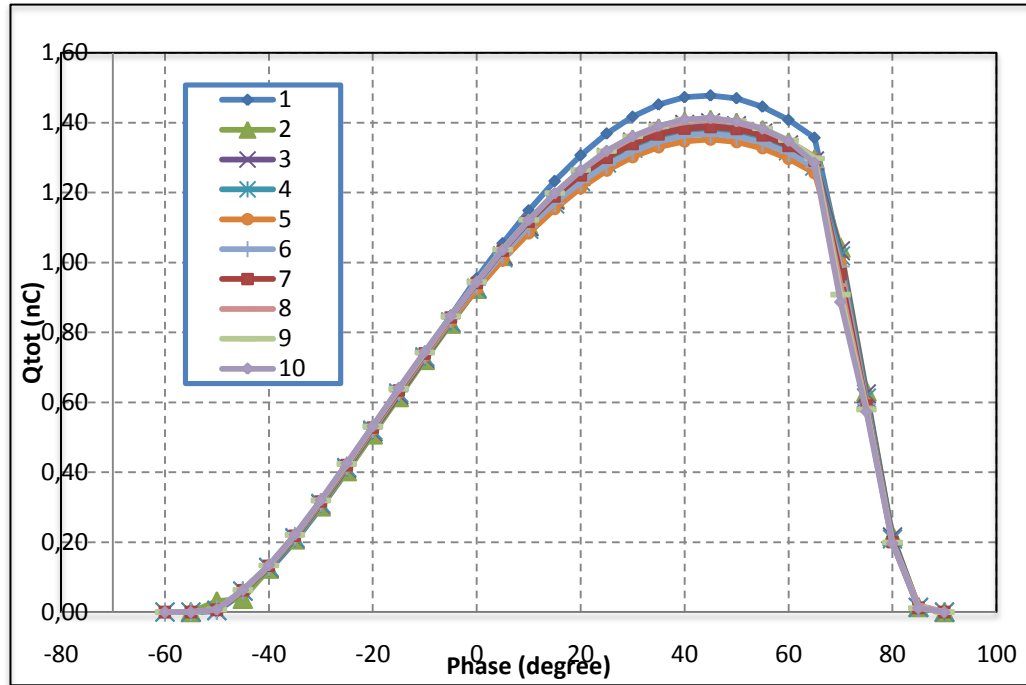


Figure 5: Phase Scan

5.2. Keep constant cathode laser intensity (Q_{bunch})

Now, we keep constant the value of Q_{bunch} equal 0.62 nC (arbitrary reasons) and we modify Q_{schottky} with 0.01 nC as step size, from 0.01 nC to 0.1 nC. Phase interval is the same as before. As mentioned above, this allows us to understand to what extent the results are modified due to the Schottky effect. The results are presented below.

Nr	Q_{bunch} (nC)	Q_{Schottky} (nC)
20	0.62	0.01
21	0.62	0.02
22	0.62	0.03
23	0.62	0.04
24	0.62	0.05
25	0.62	0.06
26	0.62	0.07
27	0.62	0.08
28	0.62	0.09
29	0.62	0.1

Table 2

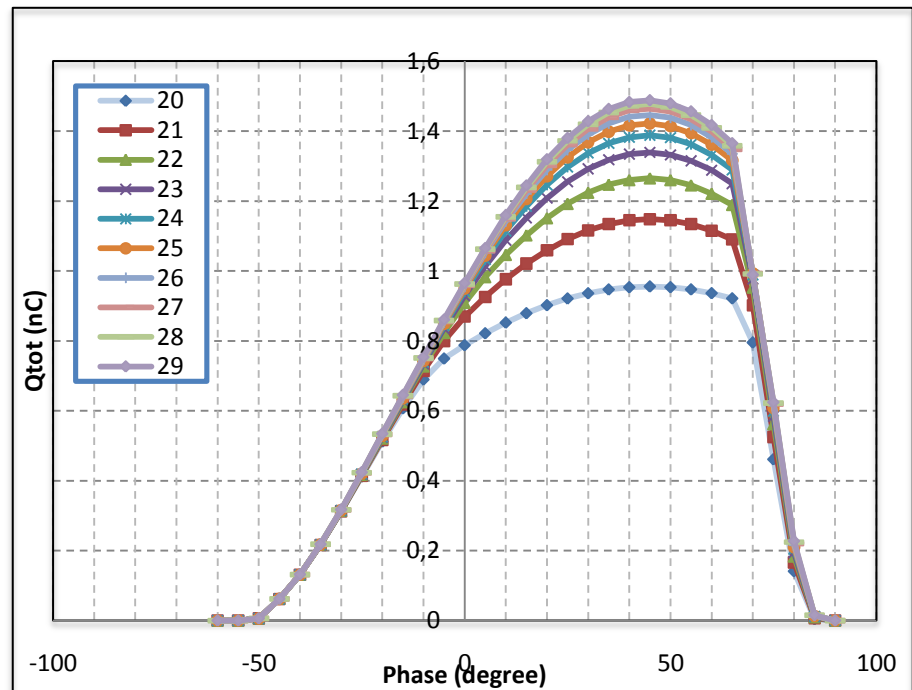
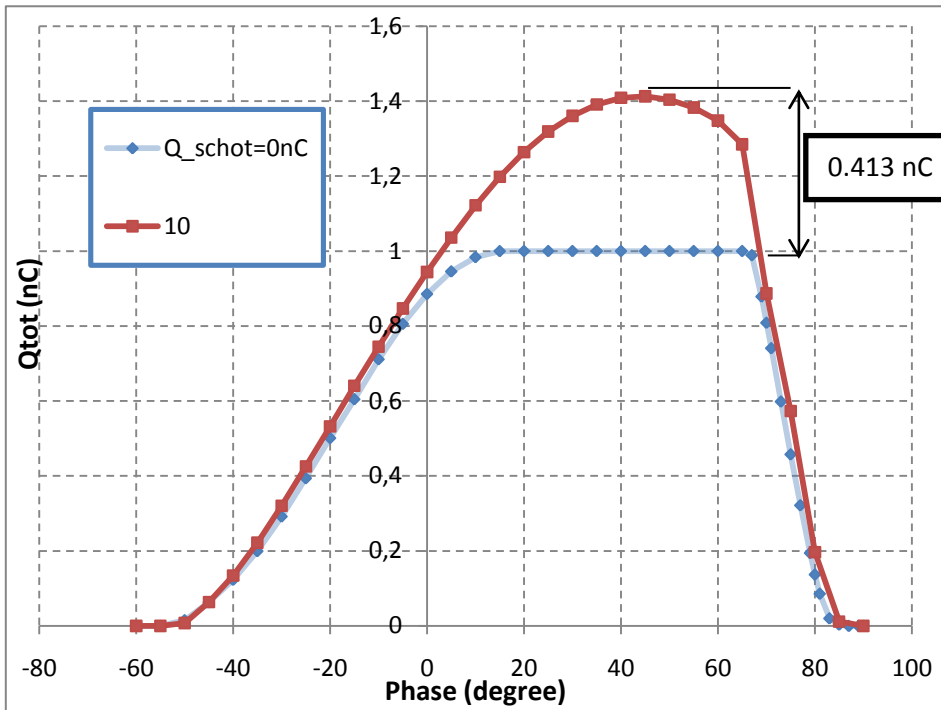


Figure 6: Phase scan keeping constant Q_{bunch} equal 0.62 nC



As can be seen, an increase in the values of Q_{schotty} causes an increase in the final beam charge as well.

Thereafter, is presented a graph which represents the behavior of the beam charge when the Schottky effect is null and bunch charge is increased to 1 nC. (Figure 7, dotted blue line).

Figure 7: Comparison with and without Schottky effect

The conclusion we can draw from this graph is that if we neglect the Schottky effect the maximum beam charge that can be obtained as a result will be, exactly, that we bring initially.

Another interpretation can be deduced might be that the Schottky effect impacts not only the bunch charge but also the beam emittance at the cathode (intrinsic and slice emittance).

The second conclusion we can come is a comparison for a better understanding of how a slight variation of approximately 0.3 nC (see Nr 10 in Table 1) in Schottky charge, can change the outcome of the final charge (red solid line with markers).

The value of bunch charge is 1nC in both cases and this small difference in Schottky effect (0.034852099 nC) lead a growth of 0.413 nC

6. Comparison with experimental results

Once the first results have been obtained they should be compared with the real electron beam's behavior. In Figure 8 are shown the simulated results (Table 2) and experimental data together. In this manner we can contrast which parameters fit the best the experimental results.

In order to comparing experimental and simulated graphs both of them correspond to a value of bunch charge equal 0.62 nC.

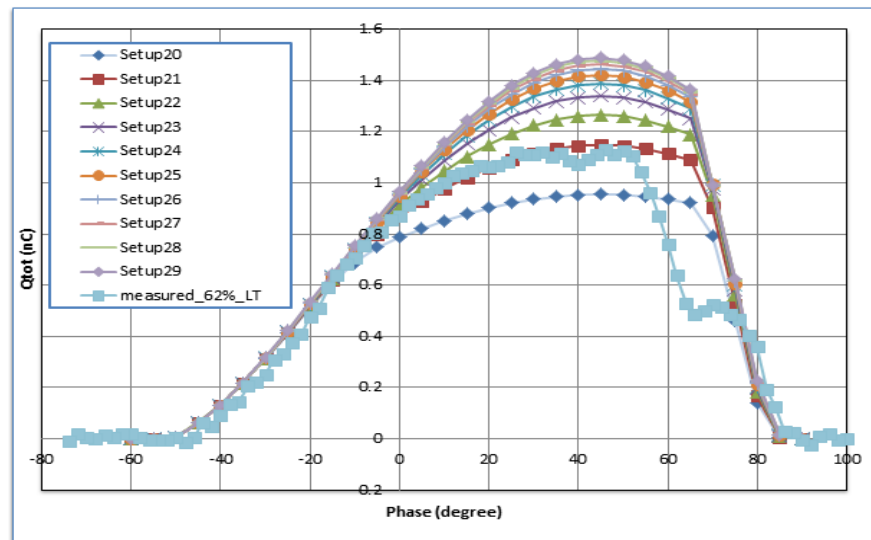
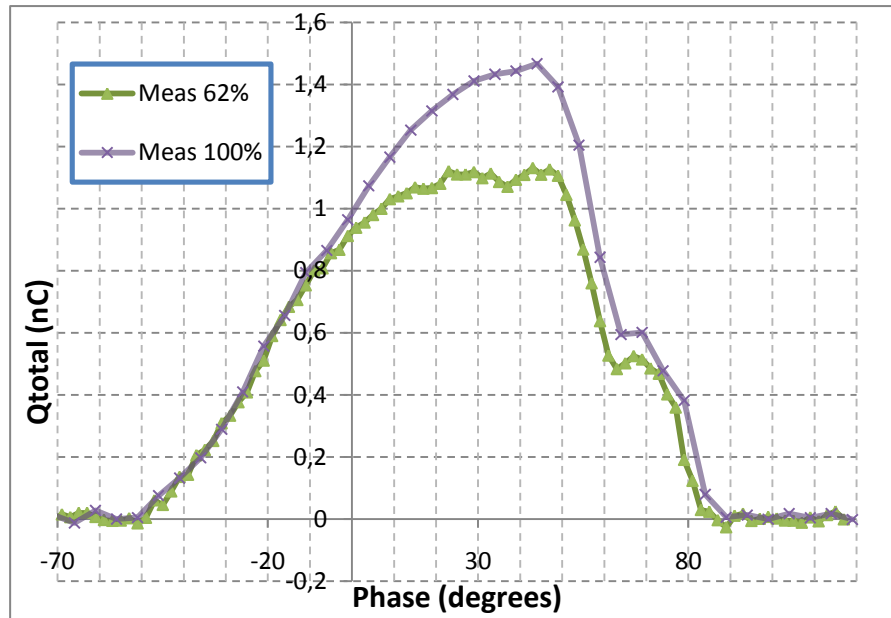


Figure 8: Comparison between experimental (measured_62%_LT) and simulated results. $Q_{\text{bunch}}=0.62\text{nC}$

Seems obvious that *Setup21* (red dotted line, which corresponds to Nr. 21 in Table 2, can be chosen as the best, compared with the experimental data. Only between 50 and 75 degrees the differences are ostensibly evident, the only reason is that no beam line aperture has been used.

Figure 9: Experimental results associated with a 62% and 100% of transmission.



In Figure 9 are presented the experimental results corresponding to 62% and 100% transmission. Our goal will be to maintain a constant phase of 8 degrees and find $Q_{Schottky}$, $SRT_{Q_{Schottky}}$ and the beam size (XY_{rms})⁶ values that correspond to the measurements given. To do this, Q_{bunch} scan has been done varying its values between 0.1 and 2.5 nC with a 0.1 nC step (Figure 10).

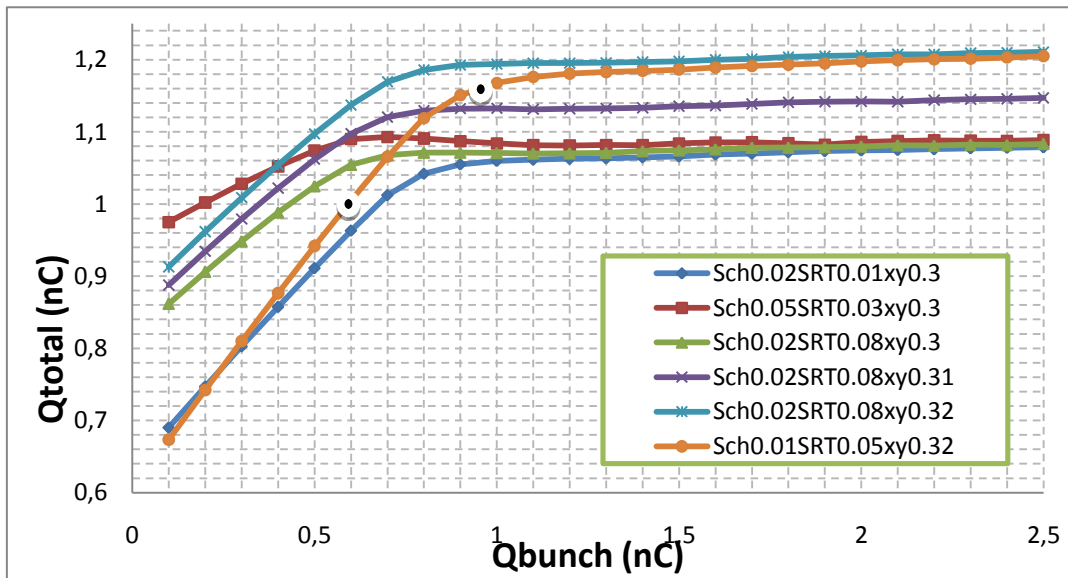


Figure 10: Q_{bunch} scan for different values of $Q_{Schottky}$, $SRT_{Q_{Schottky}}$ and XY_{rms} .

⁶horizontal and vertical root mean square beam size

Selected orange plot in *Figure 10*, is the only combination of parameters ($Q_{Schottky}=0.01nC$, $SRT_{Q_{Schottky}}=0.05nC$ and $XYrms=0.32mm$, beam size had to be increased in a 6% to achieve the experimental results) which meets the experimental results found, that means 1 nC for 62% of transmission and 1.16 nC for 100% transmission at the same phase (see *Figure 3*). In this case the results which have been found were 0,595 nC of Q_{bunch} for 1 nC of Q_{total} and 0.959677 nC of Q_{bunch} for 1.16 of Q_{total} after applying $*100/62*$ factor (see the black over white dots at the orange line in *Figure 10*).

It was necessary not only to modify the values of the charges ($Q_{Schottky}$ and $SRT_{Q_{Schottky}}$), even also the value of the rms beam size, which can be interpreted as the beam diameter divided by four ($D/4$).

Introducing these values in ASTRA can be simulated another phase scan and the results are shown below (*Figure 11*). These reproduced results fit perfectly the experimental ones, except in the area of secondary emission, 60-80 degrees approximately. The ASTRA file responsible of the secondary emission process is not implemented in this study; the area where is focused this article is around 0-10 degrees, that means, first electron emission process, so we can ignore the differences detected in secondary emission environs.

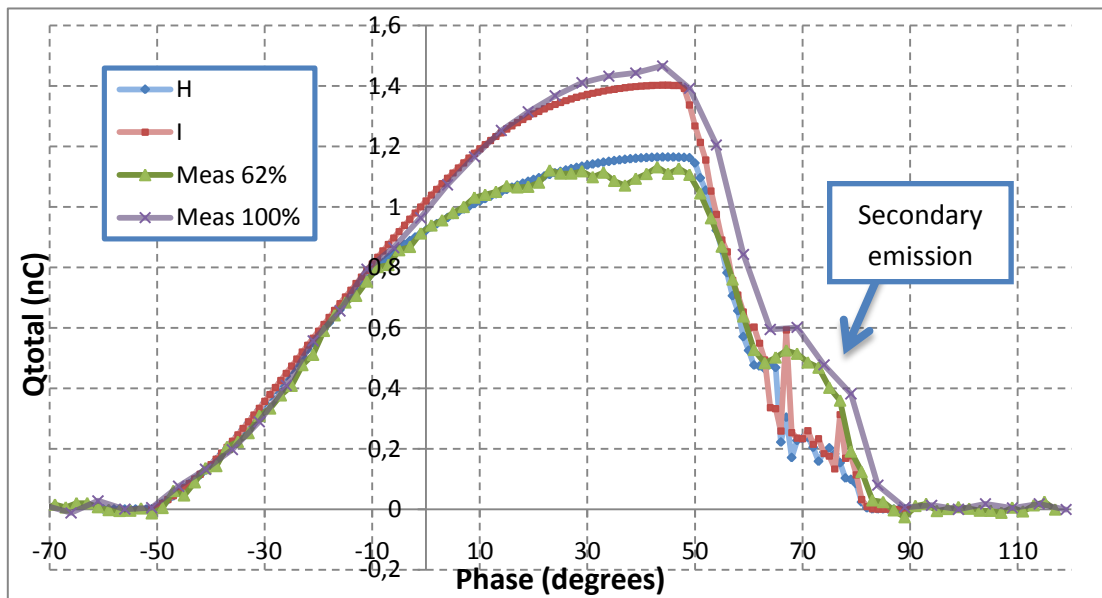


Figure 11: Phase scan. Comparison between experimental and simulated results.
H: $Q_{Schottky}=0.01nC$; $SRT_{Q_{Schottky}}=0.05nC$; $Q_{Bunch}=0.595nC$; $XYrms=0.32$
I: $Q_{Schottky}=0.01nC$; $SRT_{Q_{Schottky}}=0.05nC$; $Q_{Bunch}=0.959677nC$; $XYrms=0.32$

7. More accurate modeling of the cathode transverse distribution

The last step to completing the road that we had set at the beginning of the article, several pages ago, is to consider the relevance that may have the halo and how it behaves in the electron beam creation. For this reason, the following parameters have been raised.

	Main beam	Halo
XYrms (mm)	0.28	0.41
Total Charge ⁷ (%)	74	26
no. electrons	100000	100000

⁷Total Charge is considered uniformly distributed.

An application *postpro.exe* included in ASTRA code allows representing and studying the following aspects of electron beam and halo behavior. The results are shown below. On the one hand, the experimental on lasers temporal profile and transverse distribution are presented.

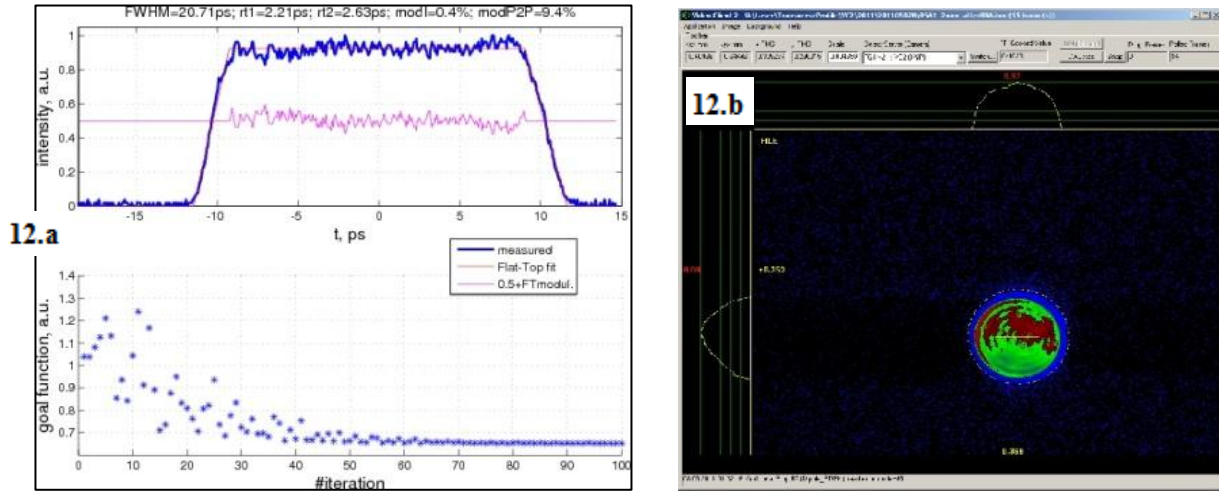


Figure 12: Measurements 08.05.2011N. Beam and halo.

Figure 12.a, shows the temporal laser profile and the intensity distribution. In the Figure 12.b is observed how the intensity distribution of the cathode laser is not uniform (green and red colors) and also is seen the narrow halo around the mean beam (blue ring). In the *Cathode laser beam halo modeling* section, the simulated results are also presented so we can compare the differences and the similarities that exist.

Below, are presented the homogeneity ASTRA distributions and after that the results which were obtained considering halo appearance.

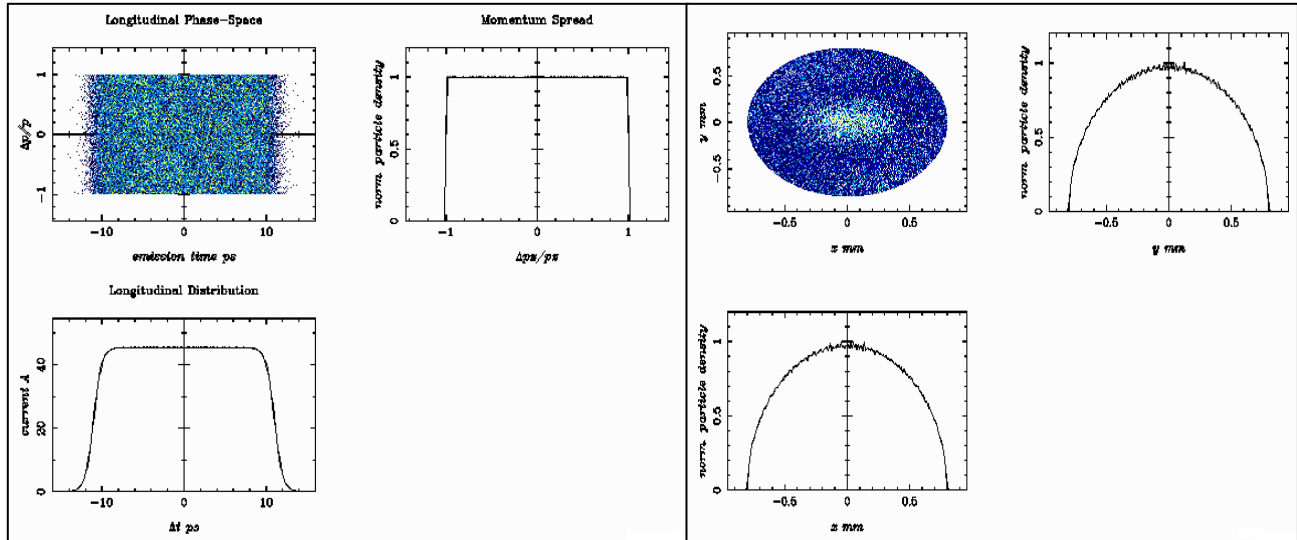
In the first plot, *Longitudinal phase-space*, is plotted $\Delta p/p$ against emission time (ps). The homogeneous case is clearer than the other case, the colors are sharper when the halo does not appear and only the mean beam is registered. However, the temporal profile in both cases is the same. In the latest pictures is where we can recognize the halo appearance. The dotted dark blue ring around the central sharp ellipse⁸ is the halo representation.

In homogeneous case the graphics are much clearer and the dispersion of points is much smaller. That is why, when we consider the halo appearance a percentage of the particles are dispersed in the halo, while in the homogeneous case the 100% of particles are focused in the main beam.

Finally, were added the transverse distribution projection, this allows to compare again the homogeneous and non-uniform cases. In the first case, is observed a distribution closer to a semicircle shape, while in the second case is discerned a central narrower part and then two smoothed steps, one on each side, corresponding to the halo appearance.

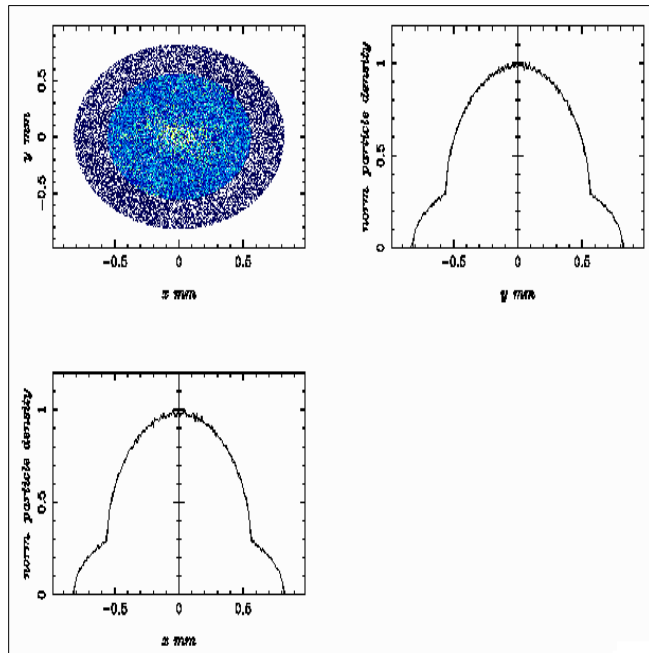
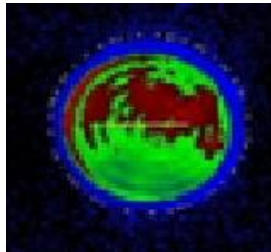
⁸Is supposed to be a circle as well as the experimental results, but the scale is modified to adjusting the plots.

Cathode laser distribution used in the simulations:



Cathode laser beam halo modelling:

Here, we can compare the experimental result taken from *Figure 12.b* with the simulations, which are uniformly distributed.



8. Conclusions

After analyzing and interpreting all the results obtained from ASTRA simulations we can extract that the objectives set at the beginning of this report and indicated on my arrival at DESY, PITZ group, have been accomplished.

The main physical concepts have been introduced and linked over all the report trying to explain how they affect the photoemission process. It has been found that in order to simulate the experimental data the following parameters have to be set into ASTRA simulation.

$XY_{rms} = 0.32$ mm, whereas 0.30 mm experimental.

$Q_{Schottky} = 0.01$ nC

$SRT_Q_{Schottky} = 0.05$ nC

It was possible to determine the simulated values which reflect as closely as possible the experimental results and they have been improved after a comparison with the outcomes from an accurate modeling of the cathode transverse distribution.

9. Acknowledgments

I would like to thank all people who have helped me during my work at DESY, especially my supervisors Mikhail Krasilnikov, Martin Khojyan and Anne Oppelt, for always finding the time to answer my questions, for supporting and advising me in every aspect of my work, sometimes leaving in the background their own labor issues. Thanks to all those are working in PITZ group for their sympathy and kindness in hosting us.

Many thanks also to Karl Jansen, Sabine Baer and all the people who have been working behind this Summer Student Program 2011 for allowing me to participate in this experience. Thank the others, Zeuthen and Hamburg, students the shared experiences living this summer and wish them the best luck in the future, professionally and personally.

Last but not least, thanks DESY personal whose work is sometimes forgotten, cleaners, cooks, security guards, always with a smile for everybody.

And finally, thanks to Jesús Daniel Santos and Javier Cuevas for recommending and encouraging me to join this great opportunity, as well as my parents, without whose support any of this would have been possible.

10. References

- [1] **K. Floettmann**, “*A Space charge Tracking Algorithm (ASTRA)*”, user manual, 1997
- [2] **M. Krasilnikov**, “*Beam Dynamics Optimization for the XFEL Photo Injector*”, p. 880, 2009
- [3] **Jang-Hui Han**, “*Dynamics of Electron Beam and Dark Current in the Photocathode RF Guns*”, p. 11-27, October 2005
- [-] **H. Qian, Y. Hidaka, J.B. Murphy, B. Podobedov, S. Seletskiy, Y. Shen, X. Yang, X.J. Wang, C.X. Tang**, “*High-Brightness Electron beam Studies at the NSLS SDL*”, National Synchrotron Light Source, Brookhaven national Laboratory, P.O. Box 5000, Upton, NY 11973
- [-] **K. Schindl**, “*Space Charge*”, CERN, CH-1211 Geneva 23
- [-] **S. Schreiber, M. Gorler, K. Klose, M. Staack, L. Frohlich**, “*Experience with the Photoinjector Laser at FLASH*”, DESY, Hamburg, Germany

